

---

# Decision-aware training of spatiotemporal forecasting models to select a top $K$ subset of sites for intervention

---

Kyle Heuton<sup>1</sup> F. Samuel Muench<sup>1</sup> Shikhar Shrestha<sup>2</sup> Thomas J. Stopka<sup>2</sup> Michael C. Hughes<sup>1</sup>

## Abstract

Optimal allocation of scarce resources is a common problem for decision makers faced with choosing a limited number of locations for intervention. Spatiotemporal prediction models could make such decisions data-driven. A recent performance metric called fraction of best possible reach (BPR) measures the impact of using a model’s recommended size  $K$  subset of sites compared to the best possible top- $K$  in hindsight. We tackle two open problems related to BPR. First, we explore *how to rank* all sites numerically given a probabilistic model that predicts event counts jointly across sites. Ranking via the per-site mean is suboptimal for BPR. Instead, we offer a better ranking for BPR backed by decision theory. Second, we explore *how to train* a probabilistic model’s parameters to maximize BPR. Discrete selection of  $K$  sites implies all-zero parameter gradients which prevent standard gradient training. We overcome this barrier via advances in perturbed optimizers. We further suggest a training objective that combines likelihood with a decision-aware BPR constraint to deliver high-quality top- $K$  rankings as well as good forecasts for all sites. We demonstrate our approach on two where-to-intervene applications: mitigating opioid-related fatal overdoses for public health and monitoring endangered wildlife.

models that can make accurate predictions of near-term future events at fine spatiotemporal resolutions. Such models can enable stakeholders to make data-driven decisions about how to allocate limited resources to maximize utility.

In this work, we are interested in helping decision-makers select *where to intervene*. That is, given historical data for a fixed set of  $S$  candidate spatial sites, recommend a specific subset of given size  $K$  for some kind of action or intervention. We think of hyperparameter  $K$  as setting the budget for interventions. In an ideal world, decision-makers could afford interventions in all  $S$  sites. However, when resource constraints allow only  $K$  sites to receive interventions, a decision selecting a specific  $K$ -of- $S$  subset is required. While such decisions may often be heuristic in practice, we hope to offer data-driven solutions.

With this goal in mind, choosing a sensible performance metric is critical to assessing which models have real-world utility. Common metrics such as squared error or absolute error are not well matched to where-to-intervene decisions because they treat all sites equally. Recent work on overdose forecasting has suggested a metric termed the *fraction of best possible reach*, or *BPR* (Heuton et al., 2022; 2024). BPR measures a ratio of event counts, where the numerator sums over the model’s recommended  $K$  sites while the denominator sums over the best possible  $K$  selected in hindsight. This type of evaluation has been used in a preregistered trial (Marshall et al., 2022a) for assessing forecasts of opioid overdoses in Rhode Island, as well as a follow-up feasibility study (Allen et al., 2023). BPR is applicable to many where-to-intervene problems beyond public health.

## 1. Introduction

Statistical machine learning methods for spatiotemporal forecasting can play a vital role in high-stakes applications from mitigating overdoses in public health (Marks et al., 2021b) to forest fire management (Cheng & Wang, 2008) to wildlife monitoring (Golden et al., 2022; Hefley et al., 2017). Across these domains, there is a pressing need for predictive

While some publications have reported BPR in evaluations, we suggest that a natural goal would be for this performance metric to inform two other key parts of data-driven decision-making: model-based *ranking* and model *training*. By ranking, we mean that given fixed model parameters, the knowledge of BPR as the metric of interest should impact the numerical score assigned to each site to determine the top  $K$ . By training, we mean how to update model parameters to achieve good BPR. This paper contributes new methods for solving both ranking and training problems

---

<sup>1</sup>Department of Computer Science, Tufts University, Medford, Massachusetts, United States <sup>2</sup> Department of Public Health and Community Medicine, Tufts University School of Medicine, Boston, Massachusetts, United States. Correspondence to: Kyle Heuton <kyle.heuton@tufts.edu>.

Code: <https://github.com/tufts-ml/decision-aware-topk/>

when BPR is the preferred metric.

Our work overcomes two key technical barriers. The first barrier is in ranking. Given a fixed probabilistic model, determining how to compute a per-site score that is sorted to find the top  $K$  is not obvious. It may be tempting to use the model’s per-site mean, but decision theory suggests different loss functions usually have distinct corresponding best estimators (Berger, 2013; Murphy, 2022). As a relatively new metric, the problem of how to assign a numerical ranking to sites for optimal BPR decision-making is currently open. We contribute a tractable ranking method that is provably best for a reasonable bound on BPR. We further show how the *score function estimator* (Kleijnen & Rubinstein, 1996; Mohamed et al., 2020) can be used to calculate gradients of this ranking with respect to parameters.

The second barrier prevents training parameters to improve BPR. First-order gradient descent enables training of many prediction methods, yet gradients of BPR with respect to parameters are problematic. The selection of the recommended top  $K$  sites is piece-wise constant function of model parameters. While small changes to parameters will induce small changes per-site scores, only changes large enough to move a site into or out of the top- $K$  ranked sites will have an affect on BPR. Thus, gradients of BPR with respect to parameters will be zero almost everywhere, preventing gradient methods from ever moving beyond subpar initial parameters. To fix this, we leverage recent advances in *perturbed optimizers* (Abernethy et al., 2016; Berthet et al., 2020) to yield effective and efficient gradient estimation for BPR. Our team explored this idea for optimizing BPR alone in earlier non-archival work (Heuton et al., 2023); this paper offers an expanded treatment with more accessible presentation. Yet optimizing BPR alone can lead to model predictions with far lower likelihood than conventional training, leading to concerns about overall model quality and generalization. To address this, we further pose a constrained optimization problem to maximize likelihood subject to a BPR quality constraint that delivers quality top- $K$  recommendations *and* good forecasts for all sites.

We ultimately contribute methods for how-to-rank and how-to-train when making where-to-intervene decisions. Using these tools, a variety of models can be directly optimized to make effective top  $K$  site recommendations. We demonstrate these contributions first on synthetic data, where we reveal how off-the-shelf methods without our innovations can be suboptimal for decision-making. We further offer evaluations of two real applications: mitigating opioid-related fatal overdoses and monitoring endangered birds.

Throughout this paper, a recurring takeaway message is that conventional training methods based on maximizing likelihood can yield suboptimal decision-making for BPR, especially when forecasting models are misspecified. In

this vein, our work shares the same broad goals as *direct loss minimization* (Wei et al., 2021) and *loss-calibrated methods* (Lacoste-Julien et al., 2011). We are inspired by the way these works bring utilities (losses) and Bayesian decision theory to improve training of probabilistic methods. Others have extended loss-calibrated methods to neural nets (Cobb et al., 2018) and to continuous (not discrete) actions (Kuśmierczyk et al., 2019). Yet a tractable and scalable recipe specifically for BPR-like objectives that prioritize  $K$ -of- $S$  decision-making is not an immediate next step from this past work. We hope our contributions spark interest in where-to-intervene problems in the methodological community and also lead to effective deployments of data-driven top- $K$  decision-making in public health and beyond.

## 2. Technical Background and Problem Setup

**Notation.** Mathematically, some of our notation follows Sander et al. (2023). Function TOPKMASK takes as input a vector  $\mathbf{r}$  of length  $S$  and an integer  $K$ . It produces a binary vector of length  $S$  with exactly  $K$  entries equal to 1. Each 1 entry corresponds to a value in the top  $K$  largest entries of the input vector. The  $s$ -th entry of the output is

$$\text{TOPKMASK}(\mathbf{r}, K)_s = \begin{cases} 1 & \text{if } \text{RANK}(\mathbf{r})_s \leq K \\ 0 & \text{otherwise} \end{cases}, \quad (1)$$

Here, function RANK provides a numerical ranking (largest-to-smallest) from 1 to  $S$  for each entry of an  $S$ -dimensional input vector. The function TOPKIDS acts on the same input as TOPKMASK, but return the size  $K$  set of integer indices corresponding to top  $K$  values.

**Problem definition.** We wish to probabilistically model events that occur across  $S$  distinct spatial sites over time. At each site, indexed by  $s$ , we can observe a *non-negative* scalar count or value  $y_s \geq 0$ . We assume that larger  $y_s$  corresponds to greater value in intervention at site  $s$ . In our public health applications,  $y_s$  represents counts of fatal overdoses. In our later wildlife monitoring case study,  $y_s$  counts how often a rare animal appears. At each time  $t$ , we stack all observations into a vector  $\mathbf{y}_t \in \mathbb{R}^S$ .

Denote our joint model for this vector as  $p_\phi(\mathbf{y}_t)$ , where model parameter vector  $\phi$  defines the density over r.v.  $\mathbf{y}_t$ . We assume that explicitly evaluating this pdf and sampling values of  $\mathbf{y}_t$  are both feasible. Given these assumptions, our framework is quite flexible: the vector  $\phi$  could represent the weights of a neural network or the coefficients of a logistic regression or a Bayesian hierarchical model.

Our goal is to use this probabilistic model to solve a where-to-intervene decision making problem. We primarily intend to use the model to numerically rank all  $S$  sites, then select the top  $K$  sites in this ranking for near-future intervention.

**Definition of BPR.** At current time  $t$ , we evaluate a model

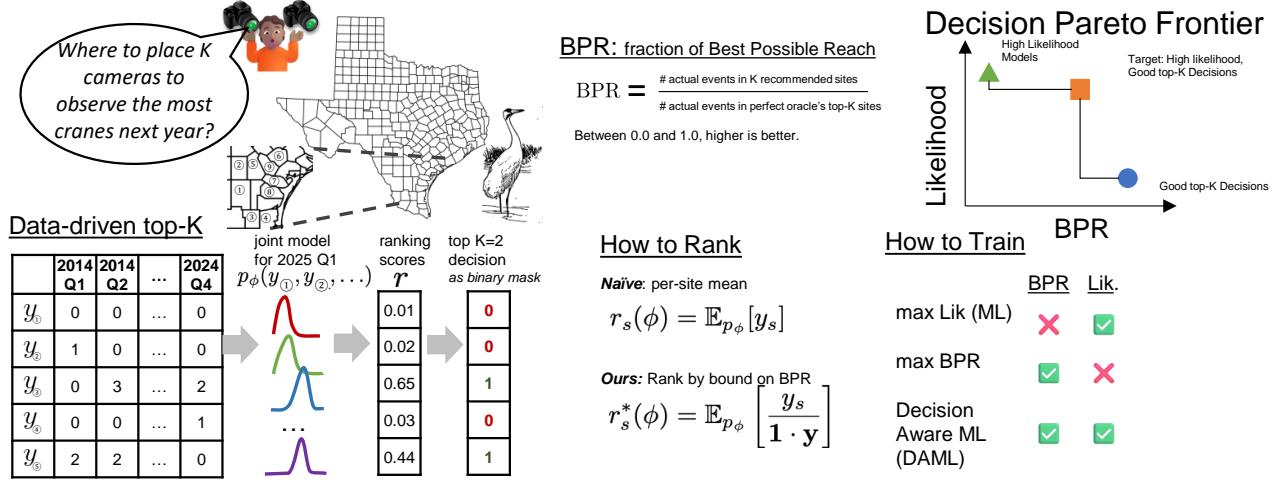


Figure 1: Visual overview of our approach and contributions to the *how to rank* and *how to train* open problems.

$\phi$ 's ability to select a top- $K$  subset of sites for intervention before time  $t+1$ . Let  $\mathcal{R}$  be the model's recommended subset of  $K$  sites among all  $S$  sites. For the rest of this section, let  $\mathbf{y} \in \mathbb{R}^S$  be the vector of observations at the target time  $t+1$  (we skip time subscripts on  $\mathbf{y}$  to keep notation simple). The vector  $\mathbf{y}$  is not available when the decision of  $\mathcal{R}$  is made. Following Heuton et al. (2022), we define BPR as:

$$\text{BPR}(\mathcal{R}, \mathbf{y}) = \frac{\sum_{s \in \mathcal{R}} y_s}{\sum_{s \in \text{TOPKIDS}(\mathbf{y}, K)} y_s}. \quad (2)$$

Both terms in this fraction can only be evaluated in hindsight, after the vector  $\mathbf{y}$  is realized at time  $t+1$ . The numerator counts how many events the model's recommendation would reach. The denominator counts how many events a perfect oracle with knowledge of the future could reach on the same budget of  $K$  sites. Overall, we interpret BPR as the fraction of events of interest the current model's selection  $\mathcal{R}$  would reach compared to perfect knowledge of the future. Higher BPR indicates a better model for choosing where to intervene. BPR's best value is 1.0, its worst is 0.0.

**Ranking sites.** Given a fixed model  $\phi$  and target time, the *ranking* problem is how to assign numerical values to all  $S$  sites so that if the top  $K$  sites are assigned to  $\mathcal{R}$ , we reap high BPR scores. We need to define a ranking vector  $\mathbf{r} \in \mathbb{R}^S$  of numerical scalar scores for all  $S$  sites. Higher  $r_s$  values indicate greater priority for site  $s$ .

Suppose we have a loss function  $L(\mathbf{r}, \mathbf{y})$  (not necessarily related to BPR) that produces a scalar value indicating the overall quality of taking an "action"  $\mathbf{r}$  and then realizing outcome  $\mathbf{y}$ . Lower values of  $L$  indicate better decisions. A natural framework for making decisions about actions (Murphy, 2022) is to minimize the expected loss:

$$\mathbf{r}^* = \underset{\mathbf{r}}{\operatorname{argmin}} \mathbb{E}_{\mathbf{y} \sim p_\phi} [L(\mathbf{r}, \mathbf{y})] \quad (3)$$

As a simplistic example, if the loss is defined as the sum of squared errors,  $\mathcal{L}(\mathbf{r}, \mathbf{y}) = \sum_{s=1}^S (r_s - y_s)^2$ , the optimal action is provably the per-site mean:  $r_s = \mathbb{E}_{p_\phi}[y_s]$ . Similarly, a loss that sums up *absolute* errors has its optimal action the per-site *median* (Schwertman et al., 1990; Balkus, 2024). We tackle defining an optimal ranking for BPR.

To pose our ranking problem formally, we need to convert the higher-is-better BPR metric into a lower-is-better loss that depends on  $\mathbf{r}$ . Define *negative* BPR loss as

$$L^{\text{BPR}}(\mathbf{r}, \mathbf{y}) = -\frac{\mathbf{y} \cdot \text{TOPKMASK}(\mathbf{r}, K)}{\mathbf{y} \cdot \text{TOPKMASK}(\mathbf{y}, K)}. \quad (4)$$

This way of writing the loss with dot products of top- $K$  binary vectors is equivalent to  $-\text{BPR}(\text{TOPKIDS}(\mathbf{r}, K), \mathbf{y})$ .

In Sec. 3 below, we show how analysis of tractable bounds of the loss in Eq. (4) suggests a high-quality ranking function  $\mathbf{r}^*(\phi)$  for BPR. This ranking is usable across different model families, as long as the model  $p_\phi$  allows generating many samples of events  $\mathbf{y}$ . Later in Sec. 4, we show how to *train* parameters  $\phi$  with gradient descent to yield better top- $K$  decisions as judged by BPR.

### 3. Methods for Ranking

**Loose bound justifies per-site mean ranking.** A natural first guess for ranking is the per-site mean:  $\bar{\mathbf{r}} = \mathbb{E}_{p_\phi}[\mathbf{y}]$ . We can show this is justifiable way to minimize expected loss on a simplistic upper bound on BPR. Assume there exists an *upper limit*  $U$  such that for all  $s$ , we can guarantee  $U \geq y_s$ . The sum over any  $K$  entries of vector  $\mathbf{y}$  in the denominator of BPR is then bounded by  $K \cdot U$ . Plugging this bound into the minimize expected loss problem and simplifying with

linearity of expectations yields

$$\mathbf{r}^* \leftarrow \underset{\mathbf{r}}{\operatorname{argmin}} - \underbrace{\frac{\mathbb{E}_{p_\phi}[\mathbf{y}]}{K \cdot U} \cdot \operatorname{TOPKMASK}(\mathbf{r}, K)}_{\leq \text{BPR}(\mathbf{r}, \mathbf{y})} \quad (5)$$

Many solutions exist: any vector  $\mathbf{r}^*$  that satisfies  $\operatorname{TOPKMASK}(\mathbf{r}^*, K) = \operatorname{TOPKMASK}(\mathbb{E}_{p_\phi}[\mathbf{y}], K)$  can be an argmin. One valid solution here is the per-site mean  $\bar{\mathbf{r}}(\phi) = \mathbb{E}_{p_\phi}[\mathbf{y}]$ . However, this solution is only optimal for a potentially quite loose bound on BPR.

#### Tighter bound suggests the ratio estimator for ranking.

Instead of bounding with constant  $U$ , we can upper bound the denominator in Eq. (4) by summing over all  $S$  terms instead of the top  $K$ :  $\sum_{s \in \operatorname{TOPKIDS}(\mathbf{y})} y_s \leq \sum_{s=1}^S y_s = \mathbf{1} \cdot \mathbf{y}$ . This bound is tighter when the sum of all entries is less than  $K \cdot U$ , which is typically true of sparse  $\mathbf{y}$  vectors in our applications. Our how-to-rank problem then becomes

$$\underset{\mathbf{r}}{\operatorname{argmin}} - \underbrace{\mathbb{E}_{\mathbf{y} \sim p_\phi} \left[ \frac{\mathbf{y}}{\mathbf{1} \cdot \mathbf{y}} \right] \circ \operatorname{TOPKMASK}(\mathbf{r}, K)}_{\leq \text{BPR}(\mathbf{r}, \mathbf{y})} \quad (6)$$

Again, we solve via any vector  $\mathbf{r}^*$  whose top- $K$  binary vector  $\operatorname{TOPKMASK}(\mathbf{r}^*, K)$  equals  $\operatorname{TOPKMASK}(\mathbb{E}_{p_\phi}[\frac{\mathbf{y}}{\mathbf{1} \cdot \mathbf{y}}], K)$ . One valid solution is the expected ratio of vector  $\mathbf{y}$  to its sum, which we nickname the *ratio* estimator

$$\mathbf{r}^*(\phi) = \mathbb{E}_{\mathbf{y} \sim p_\phi} \left[ \frac{\mathbf{y}}{\mathbf{1} \cdot \mathbf{y}} \right] \approx \frac{1}{M} \sum_{m=1}^M \frac{\mathbf{y}^{(m)}}{\mathbf{1} \cdot \mathbf{y}^{(m)}}. \quad (7)$$

This ranking is *distinct* from the per-site mean: there exist fixed models  $\phi$  where the ratio estimator and the per-site mean would select different subsets of the same  $S$  sites. See App. B for concrete cases where the ratio estimator earns BPR 2.5x to 5x higher than the per-site mean, even when all estimators know the true data-generating model.

When exact computation of this expectation is not easy, we recommend a Monte Carlo approximation using  $M$  samples  $\{\mathbf{y}^{(m)}\}_{m=1}^M$  drawn iid from  $p_\phi$ , as in Eq. (7). This is a stochastic estimator; rankings can differ across repeat trials if  $M$  is not large enough.

## 4. Methods for Training

We now consider various ways to train the parameters of our probabilistic model on a training set that covers  $T$  distinct time periods indexed by  $t$ . At each time, we have a data vector  $\mathbf{y}_t \in \mathbb{R}_{\geq 0}^S$ . Our model family in general factorizes  $p(\mathbf{y}_{1:T}) = \prod_{t=1}^T p_\phi(\mathbf{y}_t | \mathbf{y}_{1:t-1})$ . To ease notation throughout, we omit conditioning on past history or other exogenous features. So  $p_\phi(\mathbf{y}_t)$  below should be read as equal to  $p_\phi(\mathbf{y}_t | \mathbf{y}_{1:t-1})$ .

### 4.1. Maximum likelihood (ML) estimation

Conventional training would maximize the likelihood, or equivalently minimize negative log likelihood (NLL):

$$\mathcal{J}^{\text{NLL}}(\phi) = - \sum_{t=1}^T \log p_\phi(\mathbf{y}_t). \quad (8)$$

We assume  $p_\phi$  is differentiable, so solving for a point estimate  $\phi$  is possible via gradient descent. If we add an optional prior term  $\log p(\phi)$  to enforce an inductive bias or control over-fitting, this is known as *MAP* estimation.

If the model is *well-specified* and training set size  $T$  is large enough, this is a reliable strategy to estimate  $\phi$ . We could then use the ranking methods from Sec. 3 for where-to-intervene decisions. However, popular wisdom reminds us that “all models are wrong” in some way for real-world data. As we will show in later experiments, fitting a *misspecified* model via ML estimation can produce  $\phi$  that deliver suboptimal BPR, even using the optimal ranking for that  $\phi$ .

### 4.2. Direct loss minimization for BPR

Inspired by the broad goal of *direct loss minimization* (Wei et al., 2021), another approach would be to find parameters that minimize our BPR-specific decision making loss  $L^{\text{BPR}}$ . In this strategy, we seek  $\phi$  values that minimize

$$\mathcal{J}^{\text{BPR}}(\phi) = \sum_{t=1}^T L^{\text{BPR}}(\mathbf{r}_t^*(\phi), \mathbf{y}_t), \quad (9)$$

Here, for  $\mathbf{r}^*(\phi)$  we use the ratio estimator in Eq. (7).

To train with modern gradient methods, we’d need to compute the gradient  $\nabla_\phi \mathcal{J} = \sum_t \nabla_\phi \mathbf{r}_t \cdot \nabla_{\mathbf{r}_t} L_t$ . However, technical difficulties arise with each term in this chain rule expansion. Below, we propose practical estimators for each term that overcome these barriers.

**Gradient  $\nabla_\phi \mathbf{r}_t$ .** The difficulty here is differentiating through an expectation, especially when  $\mathbf{y}$  is a discrete random variable (integer counts in our overdose applications). We use the *score function trick* (Mohamed et al., 2020), popularized by Ranganath et al. (2014) yet dating back decades (Kleijnen & Rubinstein, 1996), sometimes also called REINFORCE (Williams, 1992). We can draw  $M$  samples  $\mathbf{y}_t^{(m)} \sim p_\phi$ , then compute

$$\nabla_\phi \mathbf{r}_t = \frac{1}{M} \sum_{m=1}^M \frac{\mathbf{y}_t^{(m)}}{\mathbf{1} \cdot \mathbf{y}_t^{(m)}} \nabla_\phi \log p_\phi(\mathbf{y}_t). \quad (10)$$

This estimator can reuse the  $M$  i.i.d. samples already used to evaluate  $\mathbf{r}_t$  in a forward pass. This is easy to implement for any model  $p_\phi$  where sampling and evaluating the pdf is feasible, as we have assumed. We use automatic differentiation to compute  $\nabla_\phi \log p_\phi(\mathbf{y}_t)$ .

A downside of this estimator is high variance. We mitigate this with large  $M$  values, though future work may use *control variates* (Ranganath et al., 2014; Mohamed et al., 2020)

or try complex estimators for gradients of discrete expectations (Maddison et al., 2017; Dimitriev & Zhou, 2021).

**Gradient**  $\nabla_{\mathbf{r}_t} L_t$ . For losses  $L$  defined in terms of TOPKMASK binary vectors, like BPR, it is difficult to compute useful gradients because this loss is flat almost everywhere with respect to the input rankings  $\mathbf{r}$ . To overcome this barrier, we leverage recent advances in *perturbed optimization* (Berthet et al., 2020), also referred to as stochastic smoothing (Abernethy et al., 2016). A recent computer vision method (Cordonnier et al., 2021) shows how these ideas enable selecting a top-K set of patches from a high-resolution image for downstream prediction. We adapt this top-K approach to spatiotemporal forecasting for intervention.

Concretely, Cordonnier et al. (2021) obtain tractable  $J$ -sample Monte Carlo estimates of both the top-K indicator vector  $\mathbf{b} = \text{TOPKMASK}(\mathbf{r}, K)$  and the Jacobian  $\nabla_{\mathbf{r}} \mathbf{b}$  needed for backpropagation. First, we draw  $J$  independent samples of a standard Gaussian noise vector of size  $S$ :  $\mathbf{z}_j \sim \mathcal{N}(0, I_S)$ . Then, we compute

$$\hat{\mathbf{b}} = \frac{1}{J} \sum_{j=1}^J \mathbf{b}_j(\mathbf{r}), \quad \mathbf{b}_j(\mathbf{r}) = \text{TOPKMASK}(\mathbf{r} + \sigma \mathbf{z}_j). \\ \nabla_{\mathbf{r}} \hat{\mathbf{b}} = \frac{1}{J\sigma} \sum_{j=1}^J \text{OUTER}(\mathbf{b}_j(\mathbf{r}), \mathbf{z}_j). \quad (11)$$

The Jacobian  $\nabla_{\mathbf{r}} \hat{\mathbf{b}}$  is an  $S \times S$  matrix, where entry  $j, k$  gives the scalar derivative  $\frac{\partial b_j}{\partial r_k}$ . The conceptual justification for the Jacobian estimator comes from Abernethy et al. (2016) and Berthet et al. (2020). Noise level  $\sigma > 0$  is a hyperparameter setting the strength of stochastic smoothing; it must be carefully selected in practice.

Putting our score-function trick and perturbed optimizer estimators together, we compute the overall gradient of loss at index  $t$  as a product of individual estimators:  $\nabla_{\phi} L_t = \nabla_{\phi} \mathbf{r}_t \nabla_{\mathbf{r}_t} \mathbf{b}_t \nabla_{\mathbf{b}_t} L_t$ . We compute the last term  $\nabla_{\mathbf{b}_t} L_t$  via automatic differentiation.

Armed with this gradient estimator, we can pursue direct minimization of  $\mathcal{J}^{\text{BPR}}$  via stochastic gradient descent methods. Stochasticity here comes from both  $M$  score function samples and  $J$  perturbation samples. For convenience and reliability, we use all  $T$  records in the training set in every estimate, avoiding minibatching over time.

When models are misspecified, directly estimating  $\phi$  to minimize  $\mathcal{J}^{\text{BPR}}$  should yield better BPR than some  $\phi'$  fit via conventional loss  $\mathcal{J}^{\text{NLL}}$ . However, *probabilistic forecasts* of near-future outcomes  $\mathbf{y}_{t+1}$  produced by BPR-trained  $\phi$  have questionable utility. Nothing in the  $\mathcal{J}^{\text{BPR}}$  objective makes  $p_{\phi}$  accurate even for  $\mathbf{y}_{1:T}$ ; only relative ranking matters.

### 4.3. Decision-aware maximum likelihood

To jointly achieve the goals of good top-K decisions and accurate forecasts across all sites, we propose to find param-

eters that solve a constrained optimization problem:

$$\underset{\phi}{\text{argmin}} - \sum_{t=1}^T \log p_{\phi}(\mathbf{y}_t), \quad \text{s.t. } g_t(\phi) \leq 0 \quad \forall t \quad (12) \\ g_t(\phi) = \epsilon + L^{\text{BPR}}(\mathbf{r}_t(\phi), \mathbf{y}_t).$$

Here,  $\epsilon$  is a desired *lower bound* on a tolerable BPR for the decision task. Function  $g_t(\phi)$  checks if the constraint is satisfied at time  $t$ , returning a non-positive value when  $\text{BPR}_t \geq \epsilon$  and a positive value otherwise. A feasible solution  $\phi$  must deliver BPR as good or better than  $\epsilon$  on the provided training set. Practitioners can set  $\epsilon$  to achieve a desired minimum value for BPR. For example, if BPR below 60% was unworkable to stakeholders, set  $\epsilon = 0.6$  to enforce  $0.6 \leq \text{BPR}$ , recalling by definition  $\text{BPR} = -L^{\text{BPR}}$ .

We call this objective *decision-aware ML estimation*, or DAML. If the model is well-specified and training data is plentiful, DAML should deliver the same parameters as ML estimation when  $\epsilon$  is low enough. However, when the model is misspecified and  $\epsilon$  is higher than the BPR delivered by ML-estimated  $\phi$ , we argue DAML’s constraint will produce better top-K decisions than ML alone, trading lower likelihood for higher BPR. Compared to direct minimization of  $\mathcal{J}^{\text{BPR}}$ , DAML can deliver similar BPR but more accurate forecasts of  $\mathbf{y}$  for all sites.

To solve in practice, we use the penalty method (Chong & Zak, 2013) to convert to an unconstrained loss:

$$\mathcal{J}^{\text{DAML}}(\phi) = \sum_{t=1}^T \lambda \max(g_t(\phi), 0) - \log p_{\phi}(\mathbf{y}_t). \quad (13)$$

This DAML formulation makes estimating  $\phi$  via gradient descent possible. Here,  $\lambda > 0$  is a nuisance hyperparameter that must be tuned. When the constraint is not satisfied, larger  $\lambda$  values force gradient updates to move parameters further in directions that might satisfy the constraint.

**Implementation.** Pseudocode for DAML training is provided in the supplement (Alg. A.1). There are several key hyperparameters. First,  $M$  and  $J$  are the number of Monte Carlo samples used during training to estimate gradients via the score function trick and perturbed optimizer method. Setting  $M$  and  $J$  larger produces lower variance estimates, but at the cost of runtime and memory. Consequently, we recommend setting  $M$  and  $J$  as high as affordable. We found setting both to 100 worked for tasks in Sec. 5.

Proper selection of  $\sigma$ , the standard deviation of the Gaussian noise in the perturbed estimator, is also vital. If too small, estimated gradients will be zero; too large will swamp out any data-driven signal for learning. In practice, we found that  $\sigma$  values a bit smaller than the largest elements of rating  $\mathbf{r}^*(\phi)$  worked well. Because our ratio estimator produces values between 0 and 1, we set  $\sigma$  between  $10^{-3}$  and  $10^{-1}$ .

## 5. Experiments and Results

Decision-aware training can benefit a variety of models in diverse problem domains. The subsections below cover toy and real applications. On each task, we fit models using all three training approaches from Sec. 4: ML estimation, BPR optimization, and DAML. We wish to verify common hypotheses throughout: (i) ML training can yield suboptimal top- $K$  decisions; (ii) direct optimization of BPR improves this at the expense of likelihood; (iii) our DAML allow navigating tradeoffs between likelihood and BPR.

**Common setup.** In each task below, for a fixed task-specific  $K$  we first train models for ML and BPR. Using their final BPR values as guidelines, we select a suitable range of  $\epsilon$  values for DAML and fit each one, intending to explore intermediate points on the two-objective Pareto frontier (Costa & Lourenço, 2015). When training each objective, we run many random initializations to convergence across a range of learning rates and other hyperparameters. We keep the model  $\phi$  from one run that best achieved its objective on a validation set (see App. C.1 for details), early stopping as needed. A model’s ultimate top- $K$  rankings can have some stochasticity. Thus, later figures show *estimated distributions* of BPR across 1000 trials of a  $M=1000$  sample Monte Carlo estimate of  $r(\phi)$ .

### 5.1. Synthetic Data

We begin with an illustrative synthetic case study chosen to highlight the trade-offs that decision-aware training allows a modeler to make when working with misspecified models.

**Task.** We create a synthetic dataset of  $S = 7$  sites over  $T = 500$  times. Integer data  $y_{ts}$  is generated i.i.d over time from a quantized Gaussian with site-specific mean and small constant variance. The first six sites have means evenly spaced between 10 and 60; the last site has a large mean of 100. Fig. 2 (top left) shows the training data.

**Model.** To show the benefits of our framework, we focus on a *misspecified model*. In particular, we model each site with a  $L$ -component positive Gaussian mixture model, with global mean and variance parameters and site-specific component frequencies:

$$p_{\phi}(y_s) = \sum_{\ell=1}^L \pi_{s,\ell} \cdot \mathcal{N}_+(y_s | \mu_{\ell}, \sigma_{\ell}^2) \quad (14)$$

Here  $\phi = \{\mu_{1:L}, \sigma_{1:L}, \pi_{1:S,1:L}\}$ . We reparameterize to unconstrained real values to make gradient-based learning possible: see App. D for details.

With  $L=7$  components, the model would be well-specified and could recover the true data-generating process. However, we focus on misspecification, so we fit with  $L=2$  components. This will hurt likelihood performance, as sites with distinct true means will need to use common means. However, we wish to show that solid top- $K$  decision-making

can still happen even with such severe misspecification.

**Experiment setup.** We use BPR with  $K = 5$  for this task. For reproducible details, including all hyperparameters, see Supp. D. We only report training set metrics here for simplicity; later tasks assess generalization to test data.

**Results and Analysis.** From results in Fig. 2, we draw several conclusions. First, training to optimize NLL alone delivers subpar BPR for this task. Second, optimizing for BPR alone yields much better BPR values, suggesting that even this misspecified model can deliver much better top- $K$  decision making than the off-the-shelf ML solution. However, BPR alone yields nonsensical likelihood values, as nothing in the objective forces  $\phi$  to be good at modeling the outcomes  $y$ , only at relative ranking of the  $S$  sites. In Fig. 2, we see how our DAML hybrid objective allows a user to traverse the Pareto frontier of likelihood and BPR by enforcing a desired threshold on minimum BPR. As the desired minimum BPR threshold increases, we can sweep the tradeoff between likelihood and BPR. Ultimately, our DAML yields the best high-likelihood, high-BPR solutions in the top-right corner of the Pareto plot.

### 5.2. Opioid-related Overdose Forecasting

**Motivation.** The ongoing opioid overdose epidemic in the United States has incurred roughly 400,000 deaths over the past two decades, with more than 100,000 fatal overdoses after April 2020 (U.S. C.D.C., 2022). Possible evidence-based interventions to mitigate overdose fatalities include the availability of fentanyl testing strips or overdose rescue medications like naloxone. These protective measures work best when directed at *small areas* that are *high-risk*, with co-incident education and support for proper follow-through. Public health agencies could use forecasting to help allocate limited resources towards the goal of harm reduction.

Several efforts across the U.S. have developed small-area forecasting models of opioid-related events (Marks et al., 2021b; Neill & Herlands, 2018). A preregistered trial for overdose reduction in Rhode Island (Marshall et al., 2022a) has used BPR-like metrics to evaluate the top- $K$  predictions of models with conventional training. This past work does not *rank* or *train* to improve BPR, as we do.

**Datasets.** We study the capabilities of different methods on two datasets of historical opioid-related overdose mortality. Our IRB provided a Not Human Subjects Research determination for analysis of this decedent data. The first dataset, *MA Fatal Overdoses*, covers opioid-related overdose deaths in the state of Massachusetts from 2001-2021. This is a private dataset provided by the MA Registry of Vital Records and Statistics. The second dataset, *Cook County IL Fatal Overdoses*, tracks opioid-involved overdose deaths in the greater Chicago area in 2015-2022. This is an open dataset

## Decision-aware training of spatiotemporal forecasting models

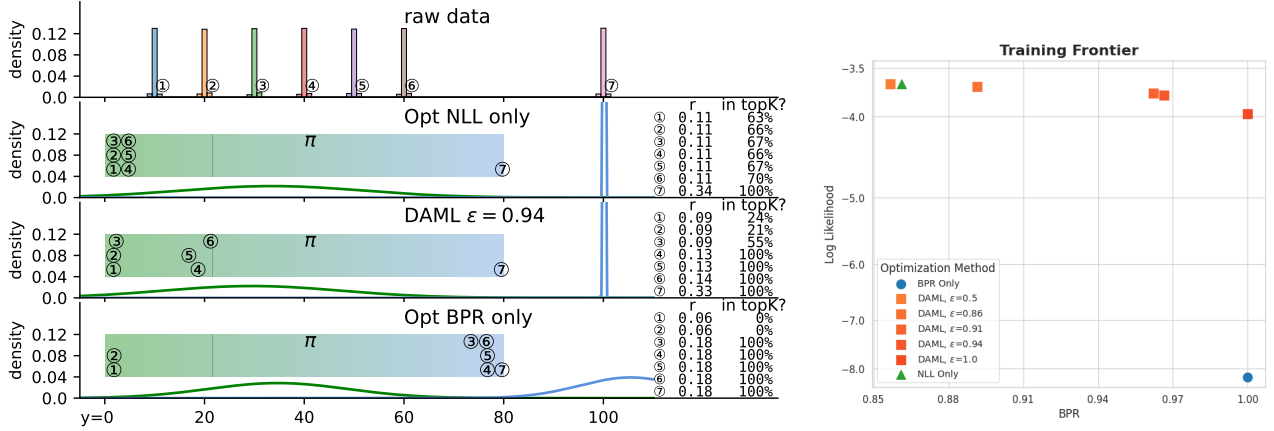


Figure 2: **Synthetic 1D data: learned models and Pareto frontier.** *Left Row 1:* histograms of  $y_s$  values by site (circled numbers). Sites 3-7 should be the top  $K=5$  under the true model. *Left Rows 2-4:* Learned Gaussian components, with site-specific weights  $\pi_s$  marked as horizontal position between pure green and blue. Text provides ranking  $r$  with how often that site is in top  $K = 5$  over 200 trials. *Right:* Likelihood vs. BPR tradeoff frontier for final models delivered by different training objectives.

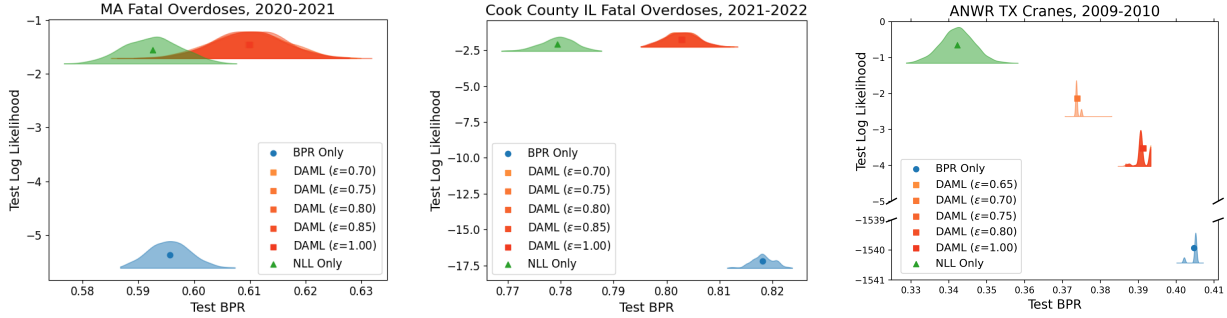


Figure 3: **Pareto frontier of best possible reach (BPR, x-axis) and log likelihood (LL, y-axis) for real-world tasks.** Higher is better on both axes. Each panel how the final models estimated by different training methods score on the test set of a forecasting task defined in Sec. 5. To capture the stochasticity of BPR due to our sampling-based ranking estimator, for each model we show an estimated density for BPR over 1000 trials. Across all 3 tasks, our proposed decision-aware ML (DAML) delivers better top- $K$  decisions as measured by BPR than ML estimation. DAML also delivers likelihood comparable to ML methods and *much better* than directly optimizing BPR.

obtained via the public website of the Cook County Medical Examiner Case Archive (Cook County, IL, 2014-present).

We follow previous evaluations of these datasets in Heuton et al. (2024). Each dataset was processed to a common format providing fatal overdose counts over time and space. For the spatial units, we chose *census tracts*. Each tract by design contains a mean population of 4000 people, a scale that allows capturing intra-municipality variation in overdoses. For temporal binning, we picked calendar years to reflect the frequency at which health agencies might enact policy changes. Summary facts are in Tab. C.1.

**Task.** Our forecasting task is to predict the next year’s count of opioid-related fatal overdoses in each census tract. For MA’s  $S=1620$  tracts, we train on data from 2011-2018, tune hyperparameters on validation data from 2019, and test on 2020 and 2021. For Cook County IL’s  $S=1328$  tracts, we train on 2015-2019, tune on 2020, and test on 2021 and

2022. These splits follow Heuton et al. (2024).

Given a trained model, we assess heldout likelihood over all sites as well as BPR with  $K=100$  to measure the model’s where-to-intervene ranking. A  $K=100$  budget was selected to reflect realistic public health budgets, and is similar to values used in other studies (Marshall et al., 2022a).

**Model.** A recent benchmark (Heuton et al., 2024) compared many models designed for overdose forecasting, including neural architectures with attention (Ertugrul et al., 2019) and more classical statistical models. A top-performer is *negative binomial mixed-effects regression* (Marks et al., 2021a). The generative model can be expressed as

$$y_{st} \sim \text{NegBin}(\mu_{st}, q), \quad (15)$$

$$\log(\mu_{st}) = \beta_0 + \beta^T \mathbf{x}_{st} + b_{0s} + b_{1s}t.$$

Here, count  $y_{st}$  is modeled as a Negative Binomial, where the log of the number of successes to stop at  $\mu_{st}$  is a lin-

ear function of feature vector  $\mathbf{x}_{st}$  as well as a site-specific intercept  $b_{0s}$  and site-specific  $b_{1s}$  weight on time  $t$ . The parameter  $q$  is a probability of success shared by all sites.

Feature vector  $\mathbf{x}_{st}$  includes tract  $s$ 's *overdose gravity*, a recent average of opioid-related overdose deaths in tracts spatially near to  $s$ , as well as measures of sociological vulnerability. See App. C.1.1 for details.

The overall parameters to estimate during training are  $\phi = \{q, \beta_0, \beta, b_{0,1:S}, b_{1,1:S}\}$ . To make constrained parameters amenable to gradient descent, we employ suitable one-to-one transforms to unconstrained spaces. Random effect weights  $\mathbf{b}$  are regularized via a *prior* that assumes a zero-mean Normal distribution with learnable covariance parameters. Full details are provided in App. E.

**Setup.** We followed the common setup described above. For reproducible details specific to overdose tasks, see App. C.1.

**Results.** Results on *test* data for both MA and Cook County IL tasks are shown in Pareto frontier plots in Fig. 3. For both datasets, we see that ML training yields suboptimal top-K decisions. Direct optimization of BPR can improve BPR, though gains on test data vary (+0.04 on Cook County; less than +0.01 on MA). Direct BPR solutions do *much worse* on likelihood, as expected. Our DAML approach provides better top-K decisions than the ML approach, with no visible decay in likelihood.

### 5.3. Endangered Bird Forecasting

**Motivation.** In the 1940s, Whooping Cranes were almost completely extinct in the U.S., with only 20 existing in the wild (Cannon, 1996). Thanks to numerous efforts over the years to preserve their population, roughly 650 cranes live in the wild today. This key species is still listed as endangered due to several threats.

A major flock of cranes, known as the Aransas-Wood population, winters at the Aransas National Wildlife Refuge (ANWR) along the Gulf Coast of Texas (Vartanian, 2023), while spending summers north in Canada. Ecologists wish to actively monitor this population. Regular aerial surveys of the Texas wintering region have been conducted for decades (Taylor et al., 2015). Using binned spatiotemporal data of sighting counts over time from these surveys, we wish to offer data-driven forecasts of where the most cranes will be. This could help stakeholders decide where to send future human monitors or where to place  $K$  fixed-location cameras to efficiently track population health.

**Data.** We use raw data from Taylor et al. (2015), which digitized decades of aerial surveys of ANWR that marked individual crane sightings on paper maps. We processed this ANWR TX Cranes data into a common format of sighting counts over time and space, selecting units to support our

goal of using the top- $K$  sites to improve monitoring. For spatial units, we divided the ANWR into 1338 boxes, each 500 meters square. A quality camera or binoculars can reasonably capture a 1.5-meter tall whooping crane in a 250-meter radius. For temporal binning, we use 2 month periods. This choice catches seasonal variation, but avoids how finer scales might burden staff to move cameras too often.

**Task.** The experiment on this data was trained on years 2002-2006, validated on 2007-2008, and tested on 2009-2010. In this context, a "year" represents one wintering season; winter 2010 means the winter that began in 2010 and ended in early 2011.

We choose  $K = 50$  for this task. This is an estimate of how many sites scientists might reasonably monitor every two months on a limited budget.

**Models.** The same negative binomial mixed-effect model was used as in Sec. 5.2. Features  $\mathbf{x}_{st}$  for site  $s$  at time  $t$  include historical bird counts at  $s$ , the latitude and longitude of the site's centroid, time of year, and the overall time.

**Setup.** We followed the common setup described above. See reproducible details in App. C.2.

**Results.** From results in Fig. 3 (right panel), we find that optimizing NLL or BPR *alone* will yield poor results in the other metric. In this case, direct optimization of BPR results in the best top-K decisions, but dramatically worse likelihood. Our DAML models improve BPR by up to 0.05 over conventional ML training with modest decay in likelihood.

## 6. Discussion

We have addressed two open challenges related to top-K resource allocation problems guided by the best possible reach (BPR) performance metric. We provided a ranking strategy that can outperform simple per-site means. We posed a training objective that strives for high likelihood across all sites while ensuring top-K decisions meet a stakeholder-specified quality level. Our experimental evaluations suggest our approach can better manage tradeoffs in likelihood and BPR than conventional training methods.

There are several limitations to this study. We focused on showing the tradeoffs between likelihood and BPR for a fixed model family in each task without comparing a wide variety of possible models. Our evaluations use fixed  $K$  values and do not explore sensitivity to  $K$  or other hyperparameters. Practitioners may need multiple metrics to assess overall utility; focusing myopically on BPR may not always be wise. Additionally, our framework assumes any site with large outcome  $y_s$  is a better candidate for intervention. Future work could explore data-driven site selection



that considers how site-specific attributes might make some interventions more or less effective.

Looking forward, we hope to see applications of these ideas inform public health, wildlife conservation, and other where-to-intervene decision-making problems across the private and public sectors. We also hope that future methodological work could scale up to much larger problems ( $S > 2000, T > 20$ ) as we found that our current experiments tested the limits of commodity GPUs.

## Acknowledgments

Authors KH, FSM, and MCH are supported in part by the U.S. National Science Foundation (NSF) via grant IIS # 2338962. Our team also acknowledges support from the American Public Health Association for a data science demonstration project. We are thankful for computing infrastructure support provided by Tufts University, with hardware funded in part by NSF award OAC CC\* # 2018149.

## Impact Statement

Recent work on where-to-intervene decision making has emphasized the importance of incorporating additional constraints into the top- $K$  site selection budget to meet the needs of all constituents. For example, Marshall et al. (2022b) sought a balance of rural and urban sites for intervention in overdose mitigation efforts in the state of Rhode Island. We believe exciting methodological work could extend the ideas in this paper to handle such constraints.

We also acknowledge that our decision-aware methods are currently technically more complex than existing off-the-shelf solutions, presenting barriers to adoption in many downstream applications where practitioners have limited hardware and limited expertise. We hope to work with stakeholders to build open-source packages that would allow DAML models to be created with off-the-shelf ease on a new dataset of interest.

## References

Abernethy, J., Lee, C., and Tewari, A. Perturbation Techniques in Online Learning and Optimization. In Hazan, T., Papandreou, G., and Tarlow, D. (eds.), *Perturbations, Optimization, and Statistics*, pp. 233–264. The MIT Press, 2016.

Allen, B., Neill, D. B., Schell, R. C., Ahern, J., Hallowell, B. D., Krieger, M., Jent, V. A., Goedel, W. C., Cartus, A. R., Yedinak, J. L., Pratty, C., Marshall, B. D. L., and Cerdá, M. Translating predictive analytics for public health practice: A case study of overdose prevention in Rhode Island. *American Journal of Epidemiology*, 2023. URL <https://doi.org/10.1093/aje/kwad119>.

Balkus, S. Proof #471: The median minimizes the mean absolute error. In *The Book of Statistical Proofs*, 2024. doi: 10.5281/zenodo.4305949. URL <https://statproofbook.github.io/P/med-mae>.

Berger, J. O. *Statistical decision theory and Bayesian analysis*. Springer Science & Business Media, 2013.

Berthet, Q., Blondel, M., Teboul, O., Cuturi, M., Vert, J.-P., and Bach, F. Learning with Differentiable Perturbed Optimizers. In *Advances in Neural Information Processing Systems (NeurIPS)*, 2020.

Cannon, J. R. Whooping crane recovery: a case study in public and private cooperation in the conservation of endangered species. *Conservation Biology*, 10(3):813–821, 1996.

CDC ATSDR. Social Vulnerability Index 2018 Database for Massachusetts., 2018.

Cheng, T. and Wang, J. Integrated spatio-temporal data mining for forest fire prediction. *Transactions in GIS*, 12(5), 2008.

Chong, E. K. P. and Żak, S. H. *An Introduction to Optimization*. John Wiley & Sons, January 2013. ISBN 978-1-118-27901-4.

Cobb, A. D., Roberts, S. J., and Gal, Y. Loss-Calibrated Approximate Inference in Bayesian Neural Networks, 2018. URL <http://arxiv.org/abs/1805.03901>.

Cook County, IL. Medical Examiner Case Archive, 2014-present. URL <https://datacatalog.cookcountyil.gov/Public-Safety/Medical-Examiner-Case-Archive/cjeq-bs86>.

Cordonnier, J.-B., Mahendran, A., Dosovitskiy, A., Weissenborn, D., Uszkoreit, J., and Unterthiner, T. Differentiable Patch Selection for Image Recognition. In *IEEE Conf. on Computer Vision and Pattern Recognition (CVPR)*. arXiv, 2021. URL <http://arxiv.org/abs/2104.03059>.

Costa, N. R. and Lourenço, J. A. Exploring pareto frontiers in the response surface methodology. In *Transactions on Engineering Technologies: World Congress on Engineering 2014*, pp. 399–412. Springer, 2015.

Dimitriev, A. and Zhou, M. Carms: Categorical-antithetic-reinforce multi-sample gradient estimator. In *Advances in Neural Information Processing Systems*, 2021. URL <https://proceedings.neurips.org>.

- [cc/paper\\_files/paper/2021/file/6e16656a6ee1de7232164767ccfa7920-Paper.pdf](https://arxiv.org/abs/2021.04714).
- Ertugrul, A. M., Lin, Y.-R., and Taskaya-Temizel, T. CAST-Net: Community-Attentive Spatio-Temporal Networks for Opioid Overdose Forecasting. In *Machine Learning and Knowledge Discovery in Databases: European Conference (ECML PKDD)*, 2019. URL [http://arxiv.org/abs/1905.04714](https://arxiv.org/abs/1905.04714). arXiv: 1905.04714.
- Golden, K. E., Hemingway, B. L., Frazier, A. E., Scholtz, R., Harrell, W., Davis, C. A., and Fuhlendorf, S. D. Spatial and temporal predictions of whooping crane (*grus americana*) habitat along the us gulf coast. *Conservation Science and Practice*, 4(6), 2022.
- Hefley, T. J., Hooten, M. B., Hanks, E. M., Russell, R. E., and Walsh, D. P. Dynamic spatio-temporal models for spatial data. *Spatial statistics*, 20:206–220, 2017.
- Heuton, K., Shrestha, S., Stopka, T. J., Pustz, J., Liu, L.-P., and Hughes, M. C. Predicting spatiotemporal counts of opioid-related fatal overdoses via zero-inflated gaussian processes. In *The 2022 NeurIPS Workshop on Gaussian Processes, Spatiotemporal Modeling, and Decision-Making Systems.*, 2022.
- Heuton, K., Shrestha, S., Stopka, T., and Hughes, M. C. Learning where to intervene with a differentiable top-k operator: Towards data-driven strategies to prevent fatal opioid overdoses. In *ICML 3rd Workshop on Interpretable Machine Learning in Healthcare (IMLH)*, 2023.
- Heuton, K., Kapoor, J., Shrestha, S., Stopka, T. J., and Hughes, M. C. Spatiotemporal forecasting of opioid-related fatal overdoses: Towards best practices for modeling and evaluation. *American Journal of Epidemiology*, pp. kwae343, 2024.
- Kleijnen, J. P. and Rubinstein, R. Y. Optimization and sensitivity analysis of computer simulation models by the score function method. *European Journal of Operational Research*, 88(3):413–427, 1996. ISSN 0377-2217. doi: [https://doi.org/10.1016/0377-2217\(95\)00107-7](https://doi.org/10.1016/0377-2217(95)00107-7). URL <https://www.sciencedirect.com/science/article/pii/0377221795001077>.
- Kuśmierczyk, T., Sakaya, J., and Klami, A. Variational Bayesian Decision-making for Continuous Utilities. In *Advances in Neural Information Processing Systems (NeurIPS)*, 2019.
- Lacoste-Julien, S., Huszár, F., and Ghahramani, Z. Approximate inference for the loss-calibrated Bayesian. In *Artificial Intelligence and Statistics*, 2011. URL [http://proceedings.mlr.press/v15/lacoste\\_julien11a/lacoste\\_julien11a.pdf](http://proceedings.mlr.press/v15/lacoste_julien11a/lacoste_julien11a.pdf).
- Maddison, C. J., Mnih, A., and Teh, Y. W. The concrete distribution: A continuous relaxation of discrete random variables. In *International Conference on Learning Representations (ICLR)*, 2017. URL <https://arxiv.org/pdf/1611.00712>.
- Marks, C., Abramovitz, D., Donnelly, C. A., Carrasco-Escobar, G., Carrasco-Hernández, R., Ciccarone, D., González-Izquierdo, A., Martin, N. K., Strathdee, S. A., Smith, D. M., and Bórquez, A. Identifying counties at risk of high overdose mortality burden during the emerging fentanyl epidemic in the USA: a predictive statistical modelling study. *The Lancet Public Health*, 6(10):e720–e728, October 2021a. ISSN 2468-2667. doi: 10.1016/S2468-2667(21)00080-3. URL [https://www.thelancet.com/journals/lanpub/article/PIIS2468-2667\(21\)00080-3/fulltext](https://www.thelancet.com/journals/lanpub/article/PIIS2468-2667(21)00080-3/fulltext). Publisher: Elsevier.
- Marks, C., Carrasco-Escobar, G., Carrasco-Hernández, R., Johnson, D., Ciccarone, D., Strathdee, S. A., Smith, D., and Bórquez, A. Methodological approaches for the prediction of opioid use-related epidemics in the United States: A narrative review and cross-disciplinary call to action. *Translational research : the journal of laboratory and clinical medicine*, 234:88–113, 2021b. URL <https://www.ncbi.nlm.nih.gov/pmc/articles/PMC8217194/>.
- Marshall, B. D. L., Alexander-Scott, N., Yedinak, J. L., Hallowell, B. D., Goedel, W. C., Allen, B., Schell, R. C., Li, Y., Krieger, M. S., Pratty, C., Ahern, J., Neill, D. B., and Cerdá, M. Preventing Overdose Using Information and Data from the Environment (PROVIDENT): Protocol for a randomized, population-based, community intervention trial. *Addiction (Abingdon, England)*, 117(4):1152–1162, 2022a. URL <https://www.ncbi.nlm.nih.gov/pmc/articles/PMC8904285/>.
- Marshall, B. D. L., Alexander-Scott, N., Yedinak, J. L., Hallowell, B. D., Goedel, W. C., Allen, B., Schell, R. C., Li, Y., Krieger, M. S., Pratty, C., Ahern, J., Neill, D. B., and Cerdá, M. Preventing Overdose Using Information and Data from the Environment (PROVIDENT): protocol for a randomized, population-based, community intervention trial. *Addiction (Abingdon, England)*, 117(4):1152–1162, April 2022b. ISSN 1360-0443. doi: 10.1111/add.15731.
- Mohamed, S., Rosca, M., Figurnov, M., and Mnih, A. Monte carlo gradient estimation in machine learning. *Journal of Machine Learning Research*, 21(132), 2020.
- Murphy, K. S. *Probabilistic Machine Learning: An Introduction*, chapter 5.1: Bayesian Decision Theory. MIT Press, 2022.

- Neill, D. B. and Herlands, W. Machine Learning for Drug Overdose Surveillance. *Journal of Technology in Human Services*, 36(1):8–14, 2018. URL <https://doi.org/10.1080/15228835.2017.1416511>.
- Ranganath, R., Gerrish, S., and Blei, D. Black box variational inference. In *Artificial intelligence and statistics (AISTATS)*, 2014.
- Sander, M. E., Puigcerver, J., Djolonga, J., Peyré, G., and Blondel, M. Fast, Differentiable and Sparse Top-k: a Convex Analysis Perspective, June 2023. URL <http://arxiv.org/abs/2302.01425>. arXiv:2302.01425 [cs, stat].
- Schwertman, N. C., Gilks, A. J., and Cameron, J. A simple noncalculus proof that the median minimizes the sum of the absolute deviations. *The American Statistician*, (1), 1990. doi: <https://doi.org/10.1080/00031305.1990.10475690>.
- Taylor, L. N., Ketzler, L. P., D., R., Strobel, B. N., Metzger, K. L., and Butler, M. J. Observations of whooping cranes during winter aerial surveys: 1950–2011. Technical report, Aransas National Wildlife Refuge, U.S. Fish and Wildlife Service, Austwell, Texas, USA, 2015. URL <http://dx.doi.org/10.7944/W3RP4B>.
- U.S. C.D.C. Underlying Cause of Death 2018–2021 by Single Race. WONDER Online Database, Centers for Disease Control and Prevention and National Center for Health Statistics, 2022. URL <https://wonder.cdc.gov/ucd-icd10-expanded.html>.
- Vartanian, J. Report on whooping crane recovery activities. 2023. URL [https://www.fws.gov/sites/default/files/documents/Annual\\_Report\\_Whooping\\_Crane\\_Recovery\\_2022\\_Aransas.pdf](https://www.fws.gov/sites/default/files/documents/Annual_Report_Whooping_Crane_Recovery_2022_Aransas.pdf).
- Wei, Y., Sheth, R., and Khardon, R. Direct loss minimization for sparse gaussian processes. In *International Conference on Artificial Intelligence and Statistics*. PMLR, 2021.
- Williams, R. J. Simple statistical gradient-following algorithms for connectionist reinforcement learning. *Machine learning*, 8, 1992.

Supplementary Material for  
Decision-aware training of spatiotemporal forecasting models

0

**Abstract**

This supplement includes additional experimental results and information for understanding and reproducing experiments.

**Contents**

<b>A Pseudocode for Training</b>	<b>13</b>
<b>B Ranking Demo for BPR</b>	<b>13</b>
<b>C Experimental Details and Results from Real-World Data</b>	<b>14</b>
C.1 Opioid-related Overdose Forecasting Results . . . . .	15
C.2 Endangered Bird Forecasting Results . . . . .	15
<b>D Experimental Details and Results from Synthetic Data</b>	<b>16</b>
<b>E Model for Negative Binomial Mixed-Effects</b>	<b>16</b>

Reproducible code used for all experiments is included in the submission’s open-source repository at <https://github.com/tufts-ml/decision-aware-topk>

## A. Pseudocode for Training

---

**Algorithm A.1** Decision-aware ML training for top-K tasks judged by BPR
 

---

**Input:**

- $\{\mathbf{y}_t\}_{t=1}^T$ , train data, each  $\mathbf{y}_t \in \mathbb{R}_{\geq 0}^S$
- $\phi \in \mathbb{R}^P$ : parameter vector for model
- $M$ : int num MC samples for score func estimator
- $J$ : int num MC samples for stochastic smoothing estimator
- $\sigma > 0$ : float stddev of stochastic smoothing estimator
- $\epsilon \in (0, 1)$ : Desired minimum BPR value. Will try to enforce constraint  $\text{BPR} \geq \epsilon$ .
- $\lambda > 0$ : Strength multiplier when constraint is violated.

**Output:** Trained model parameter  $\phi$ 
**Procedure:**

```

1: while not converged do
2:    $\nabla_{\phi} \mathcal{J} \leftarrow \mathbf{0}$  //  $P \times 1$  vector to store grad wrt params
3:   for time  $t \in \{1, 2, \dots, T\}$  do
4:      $\{\mathbf{y}_t^m\}_{m=1}^M \sim p_{\phi}$  //  $M$  Monte Carlo (MC) samples
5:      $\mathbf{r}_t \leftarrow \frac{1}{M} \sum_m \frac{\mathbf{y}_t^m}{\mathbf{1} \cdot \mathbf{y}_t^m}$  //  $S \times 1$  ranking vector via MC
6:
7:      $\mathbf{b}_t \leftarrow \text{TOPKMASK}(\mathbf{r}_t)$ 
8:      $L_t^{\text{BPR}} \leftarrow -\frac{1}{\mathbf{y}_t \cdot \text{TOPKMASK}(\mathbf{y}_t)} (\mathbf{y}_t \cdot \mathbf{b}_t)$  // Scalar loss, -BPR
9:      $g_t^{\text{BPR}} \leftarrow \epsilon + L_t^{\text{BPR}}$  // Scalar. Negative if BPR  $\geq \epsilon$  is satisfied.
10:     $\mathcal{J}_t^{\text{BPR}} \leftarrow \lambda \max(g_t^{\text{BPR}}, 0)$  // Scalar ultimate loss for BPR
11:
12:     $\nabla_{\phi} r_t \leftarrow \frac{1}{M} \sum_m [\nabla_{\phi} \log p_{\phi}(\mathbf{y}_t^m)] \frac{\mathbf{y}_t^m}{\mathbf{1} \cdot \mathbf{y}_t^m}$  //  $P \times S$  matrix, score func. est. of  $\nabla_{\phi} r_t$ 
13:     $\{\mathbf{z}_j\}_{j=1}^J \sim \mathcal{N}(0, I_S)$ 
14:     $\nabla_{r_t} b_t \leftarrow \frac{1}{\sigma} \frac{1}{J} \sum_{j=1}^J \text{OUTER}(\text{TOPKMASK}(\mathbf{r}_t + \sigma \mathbf{z}_j), \mathbf{z}_j)$  //  $S \times S$  matrix, perturbed estimate of  $\nabla_{r_t} b_t$ 
15:     $\nabla_{b_t} \mathcal{J}_t^{\text{BPR}} \leftarrow -\lambda \frac{1}{\mathbf{y}_t \cdot \text{TOPKMASK}(\mathbf{y}_t)} \mathbf{y}_t \cdot \mathbf{1}_{[g_t^{\text{BPR}} > 0]}$  //  $S \times 1$  vector, nonzero if constraint unsatisfied.
16:     $\nabla_{\phi} \mathcal{J}_t^{\text{BPR}} \leftarrow (\nabla_{\phi} r_t) (\nabla_{r_t} b_t) (\nabla_{b_t} \mathcal{J}_t^{\text{BPR}})$  //  $P \times 1$  vector
17:
18:     $\mathcal{J}_t^{\text{NLL}} \leftarrow -\log p_{\phi}(\mathbf{y}_t)$  // Scalar ultimate loss for NLL
19:     $\nabla_{\phi} \mathcal{J}_t^{\text{NLL}} \leftarrow -\nabla_{\phi} \log p_{\phi}(\mathbf{y}_t)$ 
20:
21:     $\nabla_{\phi} \mathcal{J} \leftarrow \nabla_{\phi} \mathcal{J} + \nabla_{\phi} \mathcal{J}_t^{\text{NLL}} + \nabla_{\phi} \mathcal{J}_t^{\text{BPR}}$ 
22:  end for
23:   $\phi \leftarrow \text{GRADDESCENTUPDATE}(\phi, \nabla_{\phi} \mathcal{J})$  // Use steepest descent or Adam or ...
24: end while
25: return  $\phi$ 

```

---

## B. Ranking Demo for BPR

To gain understanding about the problem of *ranking* to optimize the fraction of best possible reach (BPR) performance metric, here we present detailed analysis of a toy problem with  $S = 9$  sites. We'll assume the true data-generating process for each site is completely known throughout and that each site can be modeled independently of other sites.

$$p(\mathbf{y}_{1:9}) = \prod_{s=1}^9 p(y_s) \quad (16)$$

For each site, we select from 3 possible site-specific model archetypes, nicknamed type A, type B, and type C.

- sites #1, #2, and #3 are each iid with type A PMF

- sites #4, #5, and #6 are each iid with type B PMF
- sites #7, #8, and #9 are each iid with type C PMF

Each type’s PMF function over the non-negative integers is defined in the table below.

	Type A	Type B	Type C
	$p(y_s) = \begin{cases} 0.0 & \text{if } y_s = 0 \\ 1.0 & \text{if } y_s = 7 \\ 0.0 & \text{otherwise} \end{cases}$	$p(y_s) = \begin{cases} 0.35 & \text{if } y_s = 0 \\ 0.65 & \text{if } y_s = 10 \\ 0.0 & \text{otherwise} \end{cases}$	$p(y_s) = \begin{cases} 0.90 & \text{if } y_s = 0 \\ 0.10 & \text{if } y_s = 80 \\ 0.0 & \text{otherwise} \end{cases}$
Mean	7.0	6.5	8.0
Median	7.0	10.0	0.0

We have now defined the joint PMF  $p(\mathbf{y}_{1:9})$  over the 9 sites.

We can compare two possible ways to compute a numerical ranking of the  $S = 9$  sites:

- **Mean estimator**, which computes the per-site mean:  $\mathbf{r} = \mathbb{E}[\mathbf{y}]$
- **Ratio estimator**, which computes the expectation of  $\mathbf{y}$  normalized by its sum:  $\mathbf{r} = \mathbb{E}[\frac{\mathbf{y}}{1+\mathbf{y}}]$

For each possible ranking strategy, we repeated BPR calculations over 10000 trials. To ensure accuracy of Monte Carlo estimates, we average over  $M = 50000$  samples to estimate the expectation defining each  $\mathbf{r}$ .

Results are provided in the table below. We have two key findings. First, our proposed ratio estimator can select very different sites than the per-site mean, *even when both estimators have access to the true data-generating model*. Using  $K = 3$ , our estimator would select all type-A sites as the top 3; in contrast the per-site mean would select all type-C sites (#7-9). Second, this can produce very different BPR values. Even in this simple example, we see an absolute difference in BPR of over 0.4 between the different rankings at  $K = 1$  and over 0.39 at  $K = 3$ , which is a huge shift for a metric that is bounded between 0.0 and 1.0.

		BPR			fraction of trials each site in top $K=3$ of $\mathbf{r}$								
		$K=1$	$K=3$	$K=6$	A:#1	A:#2	A:#3	B:#4	B:#5	B:#6	C:#7	C:#8	C:#9
mean	$\mathbf{r} = \mathbb{E}[\mathbf{y}]$	0.107	0.231	0.636	0.0	0.0	0.0	0.0	0.0	0.0	1.0	1.0	1.0
ratio	$\mathbf{r} = \mathbb{E}[\frac{\mathbf{y}}{1+\mathbf{y}}]$	0.538	0.625	0.810	1.0	1.0	1.0	0.0	0.0	0.0	0.0	0.0	0.0

These results can be replicated via scripts provided in the code repository.

### C. Experimental Details and Results from Real-World Data

	# Spatial Sites	Temporal Scale	Outcomes $\mathbf{y}$	Features
MA Fatal Overdoses	1620 Census Tracts	20 years, 2001-2021	Count of opioid-related fatal overdoses	SVI, Past Deaths, Location, Time
Cook County IL Fatal Overdoses	1328 Census Tracts	8 years, 2015-2022	Count of opioid-related fatal overdoses	SVI, Past Deaths, Location, Time
Aransas TX Whooping Cranes	1338 boxes, each 500m×500m	60 years, 1952-2011 (last 10 years used)	Count of bird spotted in aerial survey	Past observations, Location, Time, Month

Table C.1: Comparison of Real datasets, in terms of number of spatial sites  $S$ , temporal scales, outcomes  $\mathbf{y}$ , and features.

## C.1. Opioid-related Overdose Forecasting Results

### C.1.1. FEATURES

The feature vector  $x_{st}$  for site  $s$  and time  $t$  includes:

- Latitude and Longitude of the centroid of the census tract  $s$
- The current timestep  $t$
- Overdose gravity, an weighted average of the prior year’s overdose deaths in all contiguous tracts. We construct the feature in the same way as (Marks et al., 2021a). Note that the original paper describes a weighted average over all regions within a radius, but the provided code uses only immediately contiguous locations. We follow the implementation from the code.
- Covariates from the Social Vulnerability Index (SVI) (CDC ATSDR, 2018). These covariates are available as 5-year estimates for every census tract in the United States and are updated every 2 years. The SVI measures report the percentile ranking of every census tract according to 4 themes: Socioeconomic, Household Composition & Disability, Minority Status & Language, and Housing Type & Transportation. We use 5 variables: each tract’s ranking in each of the four themes as well as its composite ranking.
- We include 5 temporal lags: the number of fatal opioid-related overdoses in tract  $s$  in each of the past 5 years.

### C.1.2. HYPERPARAMETER RANGES

Hyperparameter ranges explored include:

- Perturbation noise: 0.1, 0.01, and 0.001.
- Adam step size: 0.1, 0.01, and 0.001.
- Number of samples for SF estimator: 100
- Number of samples for Perturb estimator: 100
- BPR constraint  $\epsilon$ : 5 possible values of the penalty threshold: 1.0, for a threshold that always encourages better BPR, as well as 4 values selected to be around the best BPR obtained on the training data.
- Multiplier on the penalty for DAML: 30. This value was chosen so that the BPR and likelihood components were roughly the same magnitude after 100 epochs of training.

For each location, training objective (likelihood, direct loss minimization, and DAML), as well as for each threshold for the hybrid model, we selected the model based on validation dataset performance. For the maximum likelihood model and direct BPR models we picked the model that best maximized their respective objective. For the DAML models, we found that given the larger number of hyperparameter configurations, small amount of validation data, and BPR’s sensitivity, selected a model based on BPR lead to overfitting. To ameliorate this, we chose the model with the highest likelihood provided that the BPR was greater than a given threshold. Because models failed to meet the target  $\epsilon$ , we chose the BPR of the maximum likelihood model on the validation dataset as our threshold. If no models met this threshold, we selected the maximum BPR model. For the We did this by evaluating the validation performance every 10 epochs, and saving a checkpoint for the model with the lowest loss on validation data.

## C.2. Endangered Bird Forecasting Results

### C.2.1. FEATURES

The feature vector  $x_{st}$  for site  $s$  and time  $t$  includes the following variables: the past 5 count values at site  $s$ , latitude & longitude of site  $s$ ’s centroid, an enumerated timestep indicating time passed at  $t$  since the starting timestamp of the dataset, and a monthly indicator variable. The dataset includes three bimonthly periods per wintering season: Oct 20–Dec 24, Dec 25–Feb 27, and Feb 28–Apr 30. The monthly indicator received a value of 1, 2, or 3, respectively, depending on which set of months an observation spanned.

### C.2.2. HYPERPARAMETER RANGES

The same hyperparameter and model selection was performed on Whooping Crane data as the opioid experiment in Section C.1.

## D. Experimental Details and Results from Synthetic Data

**Model details.** As explained in the main paper, we use a mixture of  $L = 2$  Gaussian distributions where each is *truncated* to the positive reals. We give each of the  $S$  locations their own mixture weights  $\pi_{s,l}$  where  $\sum_{l=1}^2 \pi_{s,l} = 1$  and  $\pi_{s,l} \geq 0$ . Our model for an individual location is then:

$$p(y_s) = \sum_{l=1}^2 \pi_{s,l} \cdot \mathcal{N}_+(y_s | \mu_l, \sigma_l^2) \quad (17)$$

Our parameter vector  $\phi$  then consists of the set of all  $\mu_l, \sigma_l$  and  $\pi_{s,l}$ . We have that both  $\mu_l$  and  $\sigma_l$  should be positive, as we are modeling positive counts and standard deviation is defined to positive. To accomplish this, we transform these variables using the softplus function when performing gradient based learning. Additionally, we constrain  $\sigma_l \geq 0.2$  to avoid degeneracy. Finally, to make a valid pdf, we have that the mixture weights must sum to one:  $\sum_{l=1}^L \pi_{s,l} = 1$ . To enforce this, we transform unconstrained variables using the softmax transform. This creates a subtle issue with model identifiability, as there are many unconstrained values that will lead to similar weights, but we do not find that this impacts our ability to train models effectively to achieve good likelihood or good BPR with the appropriate objective.

**Training Procedures.** We seek to train 7 models: one that optimizes only for model log likelihood, one that optimizes only BPR-5, and 5 models penalized to achieve certain threshold values of BPR. Each model is given 20 random initializations of the model parameters. We use a learning step-size of 0.1. For models with BPR in the objective, we try a perturbation noise of both 0.01 and 0.05, with 500 samples. In the hybrid models, we use  $\lambda = 30$ , selected so that the likelihood term and the BPR penalty term are on the same order of magnitude after several epochs of training.

**Tradeoffs between likelihood and BPR when  $L=2$ .** If this model had  $L = 7$  components, it would be well-specified and recover the true data generating process. However, with only 2 components, it is forced to group locations with distant mean values, which will come at a cost to likelihood and predictive capability as assessed by BPR.

For this example, we will consider BPR-5 as our decision making metric. A model that correctly ranks the top-5 locations will achieve perfect BPR. Our misspecified model is capable of this by learning 2 distinct mean values  $\mu_k$ , one higher than the other. As long as the mixture weights for the top-5 locations  $\pi_s$  assign all probability to the high component, and the mixture weights for the bottom 2 locations assign all probability to the low component, the model will have perfect BPR.

However, this is not what the model with the best possible likelihood looks like. To maximize likelihood, a model will assign the 6 low locations to one component, and the one high location to another, as in Fig. 2.

Our hybrid objective DAML can explore the Pareto frontier between maximizing for likelihood and BPR-5. By including more locations into the high-valued component, BPR-5 will increase as log likelihood slightly decreases. Our hybrid objective formulation allows us to control this tradeoff by specifying the threshold at which the penalty term takes effect.

**Results.** Results are shown in Figure 2 in the main paper. Here we see the ability of the hybrid Decision-aware object to traverse the Pareto frontier between the best possible likelihood and BPR. The lowest threshold of 0.5 is trivially satisfied by the maximum likelihood model. The highest threshold of 1.0 is only satisfied by perfect BPR, while the 3 intermediate thresholds were chosen to explore the solution frontier that is possible by including or excluding a particular component from one of the learned mixtures. We see that by using the decision-aware training objective, we can maximize BPR while still obtaining a highly likely model.

## E. Model for Negative Binomial Mixed-Effects

Here we provide further detail on the model described in Eq. (15).

For some elements of the parameters  $\phi$ , we have a prior that informs point estimation in MAP fashion. The random effects



are assumed to follow a multivariate normal prior

$$\begin{pmatrix} b_{0s} \\ b_{1s} \end{pmatrix} \sim \mathcal{N}\left(\begin{pmatrix} 0 \\ 0 \end{pmatrix}, \Sigma\right) \quad (18)$$

where the covariance matrix  $\Sigma$  is parameterized as:

$$\Sigma = \begin{pmatrix} \sigma_0^2 & \rho\sigma_0\sigma_1 \\ \rho\sigma_0\sigma_1 & \sigma_1^2 \end{pmatrix} \quad (19)$$

Here,  $\sigma_0$  is the standard deviation of the random intercepts,  $\sigma_1$  is the standard deviation of the random slopes, and  $\rho$  is the correlation between the random intercepts and slopes, where  $-1 \leq \rho \leq 1$ . We pack these hyperparameters into a separate vector  $\eta = \{\sigma_0, \sigma_1, \rho\}$ .

**Transforming to unconstrained parameters.** To ensure parameter constraints are satisfied throughout gradient descent optimization, we employ invertible transformations that map constrained domains to unconstrained spaces. We reparameterize the correlation coefficient  $\rho \in (-1, 1)$  using  $u \leftarrow \operatorname{arctanh}(\rho)$ , allowing  $u$  to be optimized over  $\mathbb{R}$  while ensuring  $\rho = \tanh(u)$  remains within its valid bounds. For the strictly positive parameters  $\sigma_0, \sigma_1 > 0$ , we optimize unconstrained parameters  $\xi_0, \xi_1 \in \mathbb{R}$  and apply the softplus transformation  $\sigma_i \leftarrow \ln(1 + e^{\xi_i})$ , which guarantees positivity while maintaining smoothness. Similarly, for the probability parameter  $q \in (0, 1)$ , we optimize an unconstrained parameter  $\zeta \in \mathbb{R}$  and apply the sigmoid transformation  $q \leftarrow 1/(1 + e^{-\zeta})$ . During gradient descent, we optimize these unconstrained parameters, and transformed to the constrained version during forward sampling or pdf evaluation of the model.

**MAP estimation.** Together, the parameters  $\phi$  and hyperparameters  $\eta$  comprise this model. Both are point estimated to maximize the MAP objective. Thus, what is marked in the paper as NLL optimization is really best viewed as MAP or penalized NLL estimation, where the loss is

$$\mathcal{J}(\phi, \eta) = -\log p(\mathbf{y}_{1:T}|\phi) - \log p(\phi|\eta) \quad (20)$$

Similarly, when we fit this model with DAML, the above loss is what is minimized subject to the BPR constraint.